Offset-fed Slotted Antenna Practically Loaded with Split Ring as Water Quality Sensor for X-Band Industrial Applications

Atul Varshney[1], and Duygu Nazan Gençoğlan[2]

[1]ECE Department, FET, Gurukula Kangri (Deemed to be University), Haridwar-249404, Uttarakhand, India

[2] Department of Electrical-Electronics Engineering School of Electrical Engineering, Faculty of Engineering, Adana Alparslan Türkeş Science and Technology University, Adana-01250, Türkiye

Corresponding author: Duygu Nazan Gençoğlan (e-mail: dngencoglan@atu.edu.tr).

ABSTRACT This article describes the design, testing, and analysis of an offset-fed split ring-loaded slotted antenna for various water quality sensors. The antenna is designed to resonate at 10 GHz on a low-cost FR-4 substrate of dimensions $0.621\lambda_o \times 0.467\lambda_o \times 0.053\lambda_o$, where λ_o is the free space wavelength at the resonant frequency. The fabricated antenna finds excellent agreement with the measured antenna parameters. At 10 GHz, the antenna achieves a gain of 7.61 dBi, a nearly unidirectional radiation pattern, and a radiation efficiency of 76%. The research is further explored to use the antenna as a water sample sensor. The antenna is tested on various water samples by submerging it in them, and in the second scenario, contactless measurements at 10 mm away from the container's upper water level. The work examines the quality of the water by observing the shift in the resonant frequency (f_r), the antenna quality factor with different total dissolved solvents (TDS) in the water samples, and changes in the reflection coefficient (S_{11}) values. It is observed that the antenna shows less than 1.5% numerical sensitivity (NS) with f_r, and high NS with the S_{11}. The antenna's S_{11} and bandwidth vary and depending on the water sample. This antenna is suitable for X-band industrial and microwave laboratory applications.

INDEX TERMS Low-cost, Numerical Sensitivity, Offset-fed, Permittivity, Quality Factor, Slot-antenna, Split Ring, Water Quality Sensor.

I. INTRODUCTION

Many fields prefer microstrip antennas as sensor elements because of their high sensitivity, low production cost, and ease of design [1]. The commonly used fields can be considered health [2–6], industry [7–12], and food [13–20]. In addition to the sensor antennas, microwave transmission lines [21], metamaterials [22], and dielectric resonators [23] are utilized to characterize the different dielectric properties of liquid or solid materials. Microstrip antennas and microwave transmission lines are used to determine the material characteristics by analyzing the S-parameters and shift of the resonance frequencies [24]. A circular microstrip patch antenna (DMPA)-based sensor design has been implemented to detect the water content in ethanol and methanol liquids. With this sensor antenna, every 10% change in water content from 0 to 100% in ethanol and methanol liquids altered the antenna operating frequency between 2.944-2.988 GHz and 2.944-2.982 GHz, respectively [25]. In reference [26], a rectangular microstrip patch antenna with a resonance frequency of 3.87 GHz has also been designed to determine the pH level in different liquid solutions. The proposed antenna structure features a square slot with a size of 10 mm² at its center, where 0.2 ml of solution liquid samples would be dripped. It is shown that as the pH level of the liquids dropped, there are increment in the antenna's reflection coefficient and a linear decrease in the resonance frequency [26]. Another study focuses on detecting the salinity level in seawater using a microstrip antenna [27]. Different water samples with varying salt concentrations are placed in a liquid sample chamber designed between the patch and the ground plane of the antenna. Changes in the reflection coefficient and resonance frequency of the antenna are examined with different salt concentrations, where the designed sensor antenna produces 48 kHz changes in resonance frequency for every 0.01 ppt of salinity level [27]. The use of microstrip antenna-based sensors is rapidly expanding in the industry [28]. Moving parts of machines in industries and daily life often leads to friction and wear. To mitigate these wear effects, the authors typically use machine lubricants, but environmental influences can lead to moisture accumulation in these lubricants, thereby affecting their functionality. Therefore, it is necessary to determine the moisture content of machine lubricants and establish tolerable moisture levels. Thus, the authors monitored changes in the antenna's return loss (S_{11}) at a working

frequency of 2.26 GHz to detect the moisture content in lubricating oil. The microstrip transmission line serves as a sensor in the study [29]. This study aims to design a transmission line-based sensor that operates in the X-band for the detection of both legal and illegal fuels [29]. Metamaterials are artificially engineered materials with negative refractive indices and negative dielectric constants that are not naturally occurring but are produced in laboratory environments [29]. The design of the sensor incorporates voids for the dripping of fuel samples onto the transmission line. The authors talk about how the transmission value at the X-band can be seen and measured changing when different fuel samples are dripped into these holes. This makes it possible to find both illegal and legal fuels. Chuma et al. also target detecting water content in ethanol using a transmission line-based sensor [30]. In this study, the changes in the water content in ethanol alter the antenna's operating frequency between 2.25-2.40 GHz. Abdulkarim et al. designed and analyzed a metamaterial-based omega-shaped resonator transmission line sensor to test liquid samples [31]. This sensor examines samples of transformer oil, ethanol, and methanol. The goal is to determine the lifespan of transformer oil by leveraging the differences in transmission rates between aged and clean transformer oil samples. Furthermore, the study involves detecting water content in ethanol and methanol. The authors have observed that the transmission in ethanol and methanol decreased as the water content increased, while the resonance frequency increased proportionally. Furthermore, the health sector uses miniature transmission line designs operating in the 0–40 GHz frequency spectrum to detect the dielectric properties of biological fluids [32]. Dalgac et al. put the properties of biological fluids into groups by looking at changes in the dielectric constants of biological samples in the frequency domain. Another study used a metamaterial-based transmission line sensor to numerically and experimentally determine the amount of methanol in locally distilled spirits samples [33]. In a study aimed at food applications, a metamaterial-based sensor antenna with a ring resonator operating in the X-band was used to detect fatty and non-fatty milk [34]. The sensor was able to detect fatty milk at 8.64 GHz and non-fatty milk at 8.7 GHz. The 60 MHz difference between the two resonance frequencies allowed for the differentiation between fatty and non-fatty milk. Moreover, in a study by Withayachumnankul et al. focused on detecting closely dielectric constant liquids, a metamaterial-based transmission line was designed [22]. The primary component of this sensor is a discrete ring resonator (DRR), a fundamental component in metamaterials. The DRR-based sensor yields significant results correlating with changes in the transmission line's resonance frequency when contacted with the test samples. Additionally, a study aimed at detecting solid materials designed a transmission line based on a three-ring complementary split-ring resonator operating at 2.5 GHz [35]. This transmission line features an area in the center for placing samples, such as turmeric, black turmeric, mango turmeric, and deionized water. Bhatti et al. have created a sampling area in the center of this structure. TIn this area, the researchers tested samples of turmeric, black turmeric, mango turmeric, and deionized water in polypropylene tubes. These samples yield the following S_{21} measurement results: for turmeric, -11.9063 dB at 2.324 GHz; for black turmeric, -11.4268 dB at 2.288 GHz; for mango turmeric, -11.6293 dB at 2.24 GHz; and for deionized water, -13.0072 dB at 2.112 GHz. Another study designed a transmission line using discrete ring resonators operating at 5.25 GHz to detect other oils mixed with olive oil [36]. For each 10% increase, adding mustard oil samples to pure olive oil caused the resonance frequency to shift from 4.95 GHz to 4.69 GHz. Furthermore, in another study focused on liquid characterization, a high sensitivity microstrip transmission line sensor was designed [37]. Changes in the transmission rate of the microwave sensor between 1.4 and 1.6 GHz are observed with 10% increases in ethanol added to water. Even though microstrip antennas and transmission lines are used a lot in different sensing tasks, there isn't much written about how to make low-cost, offset-fed slotted split ring-loaded antennas that are specifically designed for sensing water quality. While existing studies have explored the use of microstrip antennas and transmission lines for detecting parameters such as moisture content, salinity, and dielectric properties in liquids, there remains a need for a dedicated antenna design optimized for water quality sensing with high sensitivity and accuracy. On the other hand, this study also contributes several novelties to the existing literature. The proposed offset-fed slotted split ring-loaded antenna represents a novel approach to water quality sensing. By incorporating slotted split ring loading, the antenna design offers enhanced sensitivity to changes in the surrounding medium, thereby enabling precise detection of water quality parameters. Unlike previous studies that often focused on specific frequency bands or standard antenna geometries, this research optimizes the antenna to resonate at 10 GHz, making it suitable for X-band applications. Furthermore, we carefully select the antenna's dimensions to ensure optimal performance in water quality sensing scenarios. The antenna is evaluated using various water samples, including salted water, distilled water, fountain water, and spring water. The study shows that the antenna works well in a lot of different water quality situations by looking at how it reacts to different levels of total dissolved solvents (TDS). This study introduces the concept of numerical sensitivity (NS) to quantify the antenna's sensitivity to changes in resonant frequency and reflection coefficient values. This novel analytical approach provides valuable insights into the antenna's performance characteristics, facilitating its optimization for specific sensing applications. Taking everything into consideration, the proposed study addresses a significant gap in the literature by presenting a novel antenna design tailored for water quality sensing applications, backed by comprehensive experimental validation and innovative analytical techniques. This research contributes to advancing the field of microwave sensing technology and offers promising prospects for real-

world applications in environmental monitoring, industrial processes, and healthcare diagnostics.

II. MATERIAL AND METHOD

A. WATER SENSING ANTENNA DESIGN

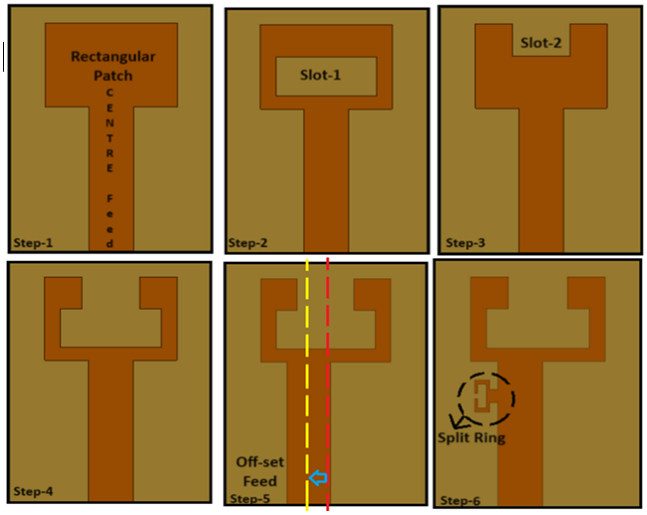

FIGURE 1. Antenna patch step-by-step development.

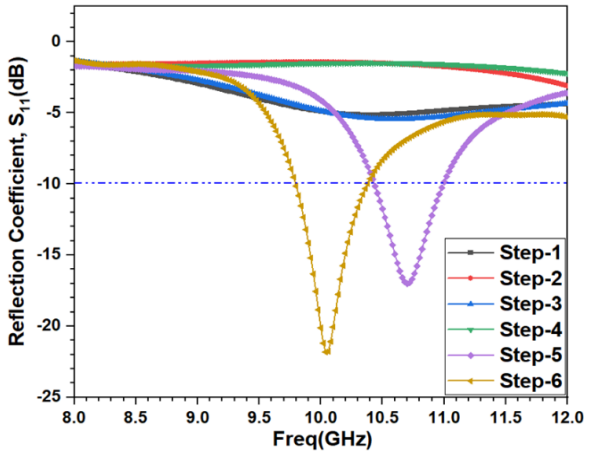

FIGURE 2. Reflection coefficient plot comparison of the antenna and patch development in six steps.

The antenna design is developed from conventional rectangular patch antenna estimation at 10 GHz with a full ground plane [38–42]. In steps 2, 3, and 4, slot-1, slot-2, and slot (slot-1+slot2) are introduced into the rectangular patch to improve the reflection coefficient values, but unfortunately, these yield no meaningful value of reflection coefficient below -10 dB. Therefore, to improve the reflection coefficient below -10 dB, the feed position is shifted (offset-feed) towards the left (step 5). This double-slotted offset-feed rectangular patch achieves a -10 dB bandwidth of 0.580 GHz (10.43 GHz–11.01 GHz) with a resonating frequency of 10.7 GHz. To improve the impedance matching and fine-tuning of the resonance frequency at 10 GHz, the slotted antenna is loaded in feed with a properly designed rectangular split ring (split gap of 0.40 mm) at 10 GHz (step 6). This practical split ring loading results in excellent impedance matching nearly at 10 GHz (0.05 GHz deviation) for a -10 dB bandwidth of 0.5785 GHz (9.7925 GHz–10.371 GHz). All the antenna development design steps are shown in Figure 1, and their resultant data are shown in Table I. Figure 2 illustrates the comparison plot of the simulated reflection coefficient of all the antenna design development steps.

TABLE I. Step-by-step water sensor antenna structure development

Design Stage	Resonance Freq., f_r (GHz)	Reflection Coeff., S_{11}(dB)	–10dB Bandwidth (GHz)	Gain, G (dBi)
Step-1	----	----	----	----
Step-2	----	----	----	----
Step-3	----	----	----	----
Step-4	----	----	----	----
Step-5	10.7	–17.02	0.580 (10.43-11.01)	4.70
Step-6	10.04	–22.463	0.5785 (9.7925-10.371)	4.92

B. ANTENNA DESIGN GEOMETRY

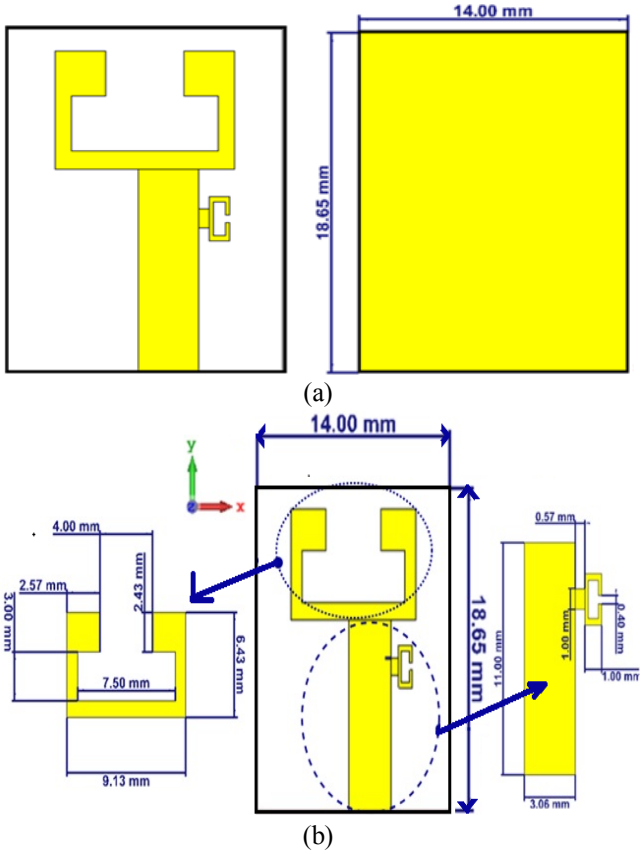

FIGURE 3. Proposed antenna (a) front and rear views, and (b) dimensional representation.

The antenna design proposed for X-band sensing applications incorporates asymmetric split-ring resonator-based radiating patches. The proposed antenna structure occupies dimensions of $0.621\lambda_o \times 0.467\lambda_o \times 0.053\lambda_o$ ($18.65 \times 14 \times 1.6$ mm^3), where λ_o is the free space wavelength at resonating frequency 10 GHz as depicted in Figure 3a. The antenna structure features a full ground plane. The upper radiating portion of the antenna is formed by a rectangular asymmetric split rectangular ring loading in feed and the proposed patch antenna is designed by cutting a pair of rectangular slots of dimensions 7.50×3.0 mm^2 (slot 1), and

4.0×2.43mm^2 (slot 2) from the conventional rectangular patch. Furthermore, we load the rectangular ring resonator into the quarter-wavelength feed line to improve resonance frequency tuning and impedance matching. Figure 3b illustrates the dimensional details of each sub-part of the proposed antenna.

C. PARAMETRIC OF SHIFTING OF OFFSET FEED

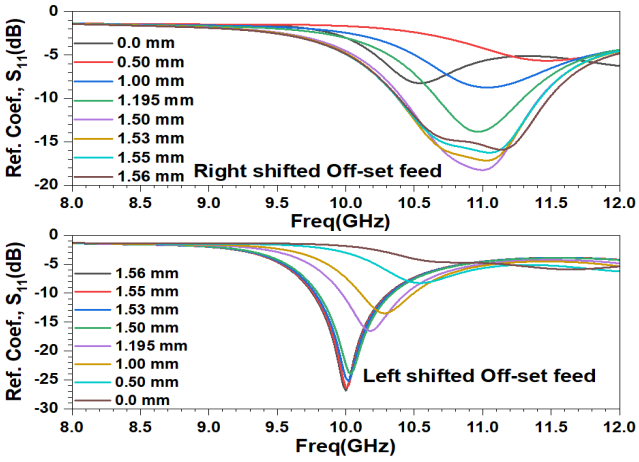

FIGURE 4. Effect of Left and Right Offset Shifting of feed.

The parametric shifting test of the offset feed of the antenna is carried out on both sides of the conventional edge feed center. Table II showcases the antenna's parametric test results, while Figure 4 compares the left shift (down) and right shift (up) feed reflection coefficients. It is noticed from Figure 4 and the recorded data in Table II that the offset left shift of the feed results in a in a resonant frequency close to the operating frequency (10 GHz resonance achieved at 1.56 mm from the feed center), and it also improves the reflection coefficients below 10 dB. On the other hand, the right offset shifting of the feed yields a wider bandwidth, a frequency shift away from the 10 GHz right side, and lowers its reflection coefficients. Therefore, the left offset shift of 1.56 mm is the optimum value [51].

TABLE II. Effect of Left and Right Offset Shifting of feed

Offset(mm)	f_0 (GHz)	S_{11} (dB)	BW (GHz)	Gain (dBi)
1.56 (left)	10.0	-26.88	9.76-10.31	7.26
1.55 (left)	10.01	-26.38	9.76-10.32	7.21
1.53 (left)	10.02	-25.20	9.77-10.33	7.22
1.5 (left)	10.04	-23.96	9.8-10.34	7.20
1.195 (left)	10.18	-16.54	9.97-10.44	7.11
1.0 (left)	10.29	-13.47	10.11-10.50	6.88
0.5 (left)	10.55	-8.26	----------	5.52
0	----------	----------	----------	3.34
0.5 (right)	----------	----------	----------	2.54
1.0 (right)	11.03	-8.75	----------	4.71
1.195 (right)	10.97	-13.85	10.67-11.30	5.32
1. 5 (right)	11.0	-18.27	10.41-11.42	5.05
1.53 (right)	11.04	-17.16	10.38-11.42	6.09
1.55 (right)	11.06	-16.26	10.38-11.42	6.17
1.56 (right)	11.14	-15.92	10.39-11.48	6.14

D. ANTENNA LOADING WITH SPLIT RING

The reflection coefficients of the effect of split ring loading and unloading cases in the feed line have analyzed in Figure 5. The left offset shifted feed antenna with 1.56 mm from feed center point is loaded with split ring in the feed. It is observed from the Table III plots recorded data that loading with split-ring the antenna in the feed not only improves the gain of the antenna but also support to resonates at 10 GHz center frequency of the X-band.

TABLE III. Simulated and measured antenna results

Antenna Loading	f_r (GHz)	S11 (dB)	-10dB BW (GHz)	Gain (dBi)
Unloaded without split ring	10.64	-37.42	10.35-10.92	6.60
Loaded with split ring	10.0	-26.88	9.75-10.32	7.26

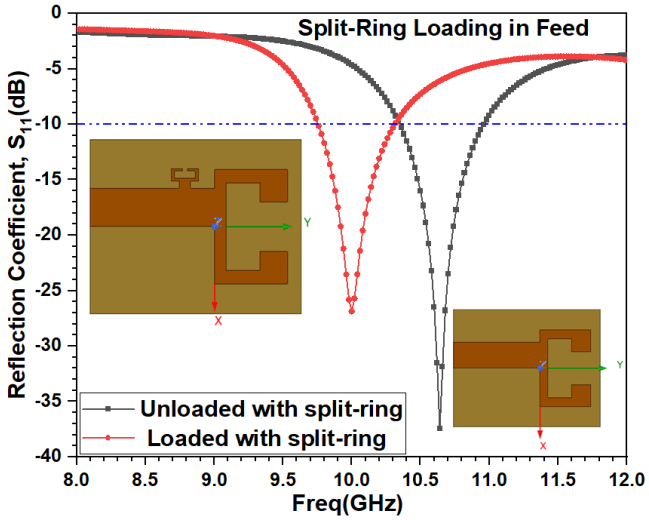

FIGURE 5. Split-ring loading in feed of antenna.

III. RESULTS AND DISCUSSIONS

In this section antenna resultant parameters validation and sensitivity analysis have been explained.

A. ANTENNA PROTOTYPE AND MEASUREMENTS

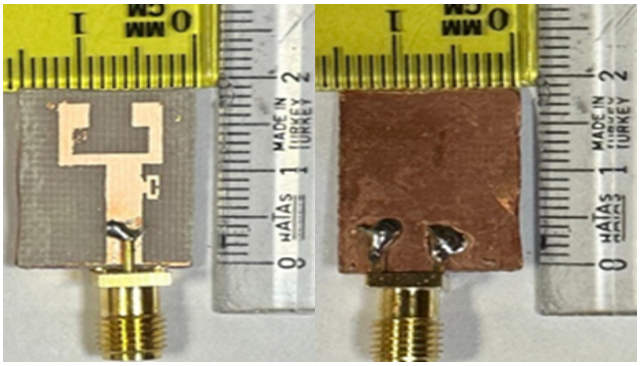

FIGURE 6. Front and rear view of Water sensing antenna.

The front and bottom views of the prototype of the water sensing antenna are fabricated by using the chemical UV exposure and etching methods, as illustrated in Figure 6. The measurement setups consist of different water samples along with a total dissolved solids (TDS) meter, and a vector network analyzer for reflection coefficient (S_{11}) measurement of the proposed antenna, which are also presented in Figures 7a to 7e to clarify the understanding of the phenomena. The main aim of this setup is to measure the S_{11} and tuning frequency sensitivities. Figure 7e shows the measurement test setups with a 0.0 mm (dipped) case.

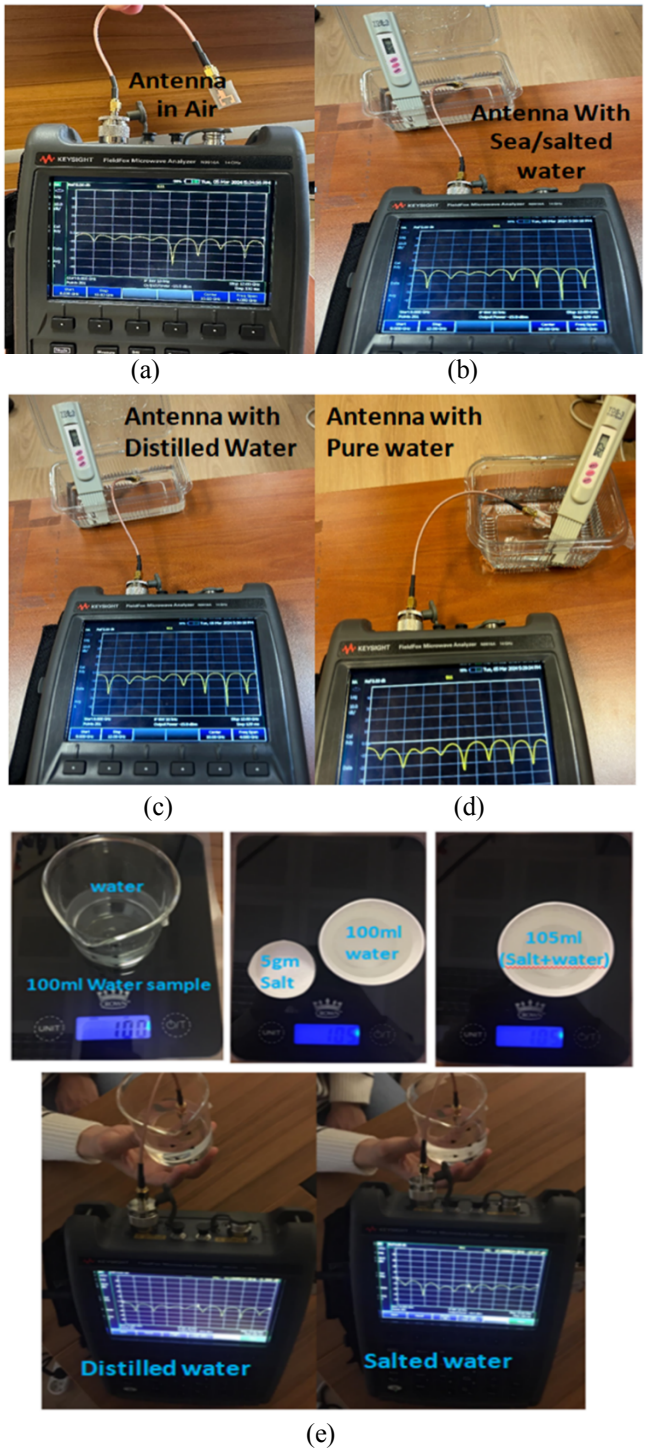

FIGURE 7. Measurement setup with 10.0mm distance (a) antenna in air, (b) antenna with seawater, (c)antenna with distilled water, (d) antenna with pure water, and (e) with antenna dipped case (0.0mm).

B. ANTENNA RESULTS VALIDATION

Figures 8a and 8b compare the simulated and measured reflection coefficient plots of the water sensor antenna. Figure 7a represents the HFSS and CST simulated results. Here, a CST-simulated antenna with similar dimensions has an almost identical resonating frequency. The HFSS antenna resonates at 10 GHz, while the CST simulated antenna resonates at 10.04 GHz with approximately the same 10 dB bandwidth. Figure 7b compares these simulated results with the measured reflection coefficients. The measured reflection coefficient resonates at 10.08 GHz, while it has a narrower (10 dB) bandwidth. These discrepancies in the results may be caused by fabrication tolerance errors in the dimensions and available material electrical properties, loss tangent variations, and soldering errors in the SMA connector. The simulated and measured results comparisons are shown in Table IV.

TABLE IV. Simulated and measured antenna results

Case	f_r (GHz)	S_{11} (dB)	-10dB BW (GHz)
Simulated HFSS	10.0	-26.88	9.75-10.32
Simulated CST	10.036	-22.76	9.79-10.39
Measured	10.08	-20.21	10.02-10.175

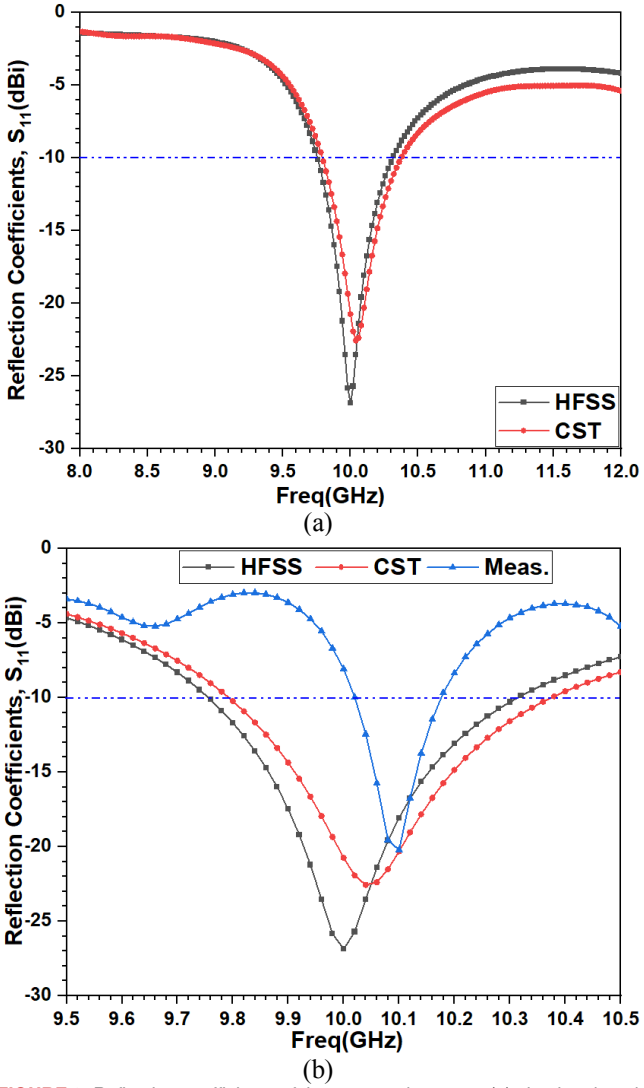

FIGURE 8. Reflection coefficients of the proposed antenna (a) simulated, and (b) simulated and measured (closed view).

C. ANTENNA RADIATION PATTERNS, GAIN, AND RADIATION EFFICIENCY

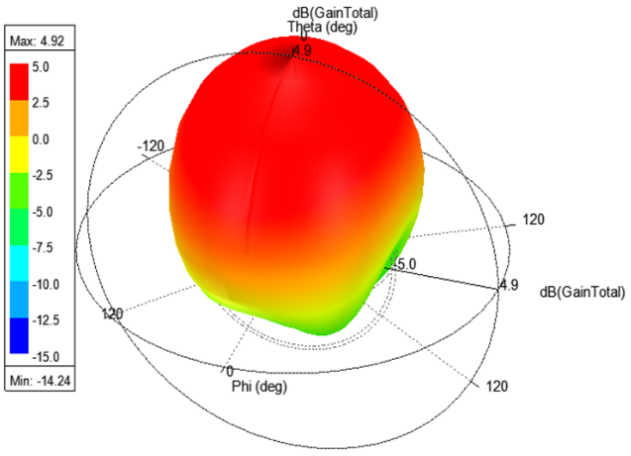

FIGURE 9. 3D radiation pattern of the antenna at 10GHz.

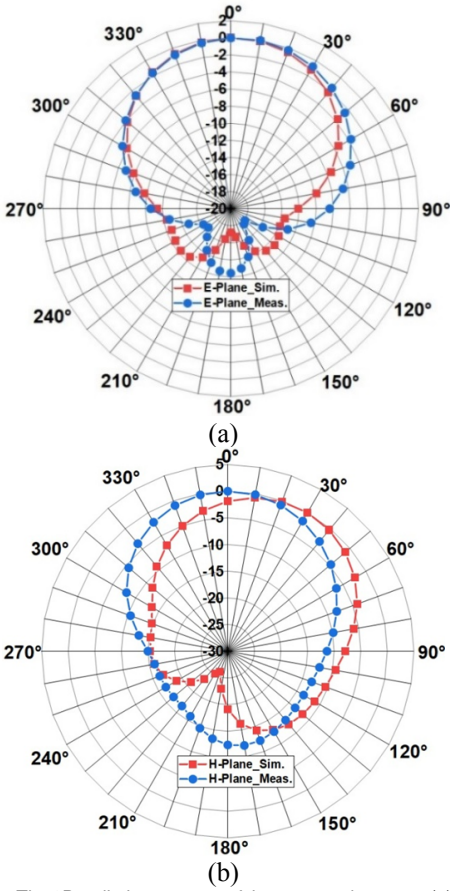

FIGURE 10. The 2D radiation patterns of the proposed antenna (a) in E-plane, and (b) in H-plane at 10GHz.

The 3D radiation pattern of the antenna is almost unidirectional in the E-plane as shown in Figure 9. The measured and simulated radiation patterns in the E-plane and H-planes are shown in Figures 10a and 10b. In both planes, gain patterns are found in excellent agreement in shape and directivity. The measured and simulated antenna gains and efficiencies are shown in Figures 11a and 11b. They were found in the same shape while the measured value of the gain and efficiencies are lacking as the antenna is designed on the lossy material FR-4 and fabrication and SMA connecter soldering errors. The antenna achieves a peak gain of 7.62dBi at the resonating frequency with a maximum radiation efficiency of nearly 76%. The discrepancies in the measured and simulated radiation patterns, gains, and radiation efficiencies results may be caused by fabrication tolerance errors in the dimensions and available material electrical properties, loss tangent variations, and soldering errors in the SMA connector. Another possible cause is the surrounding presence of any materials.

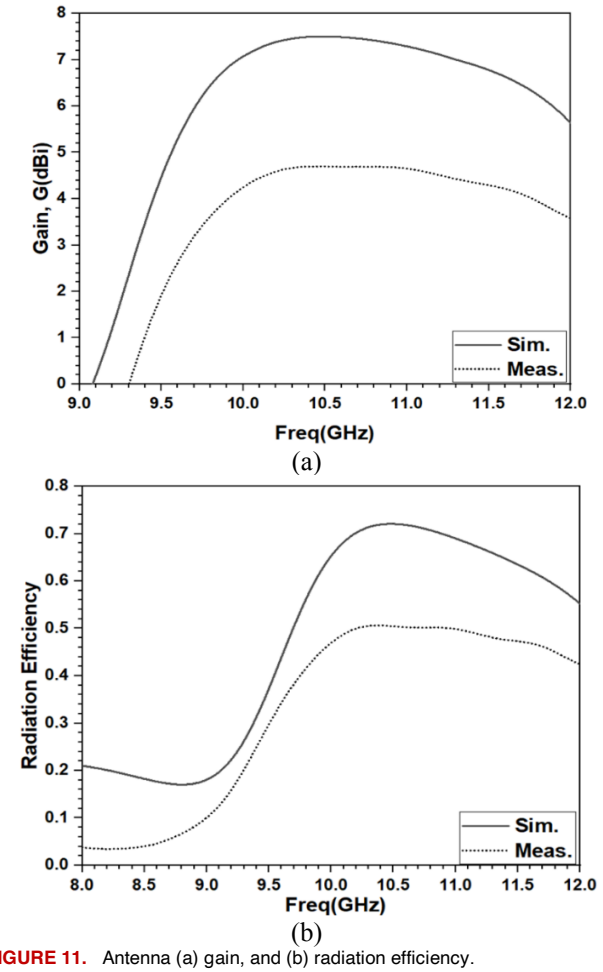

FIGURE 11. Antenna (a) gain, and (b) radiation efficiency.

D. ANTENNA CURRENT DENSITY DISTIBUTUION

The magnitude of the current density distributions of the antenna at the resonating frequency of 10 GHz are shown in Figures 12a-12b. Two cases have been considered. In case first antenna is not loaded with split-ring and in second case it is loaded with split-ring in the feed. In case first, when the antenna is not loaded with the split-ring then it shows the highest current magnitude of 221.485 A/m while when the antenna is loaded with the split-ring in its left shifted offset feed line the magnitude of the current raised excellently and it becomes 581.521 A/m. The improvement of magnitude of current is obvious because additional split-ring in feed of antenna helps to antenna resonates at 10GHz. The increased magnitude of the current density not only helps in tuning of antenna but also support to enhancement in the antenna overall gain and radiation efficiency.

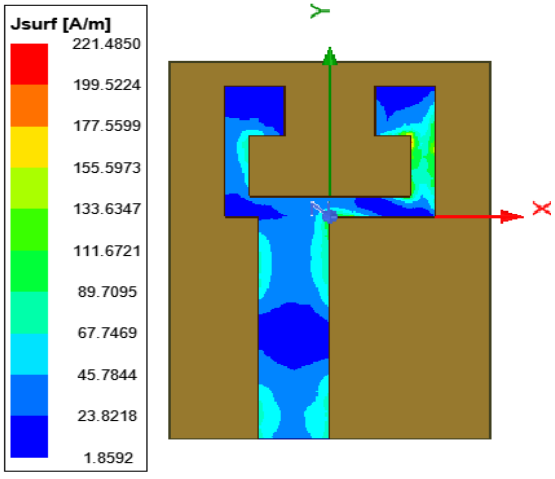

(a)

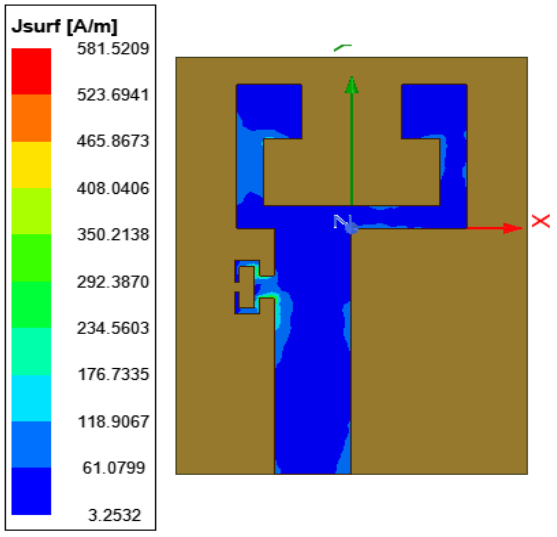

(b)

FIGURE 12. Current density distribution of antenna (a) without split ring, and (b) with split ring loading.

E. EXPERIMENTAL SETUPS IN SIMULATION SOFTWARE

The CST Microwave Studio simulation software also models the water sensing system setup using the designed antenna, as shown in Figure 13. For microwave techniques, electrical properties such as relative permittivity (epsilon), electrical conductivity (S/m), and density (rho) play a crucial role in determining how microwaves interact with different water samples. Therefore, Table V [43, 52] arranges the detailed electrical properties of each water sample.

TABLE V. Electrical properties of water samples

Water Sample	Electrical Properties at room temperature 27°C		
	Epsilon (ε_r)	Electrical Conductivity (S/m)	Rho (Kg/m^3)
Distilled	78.4	5.55×10-0.06	998
Salt (Sea)	74	3.53	1025
Pure Water	78	1.59	1000

This research set the water container cylinder's dimensions to 36 mm in diameter and 16 mm in height, and maintained a minimum sensing separation of 10 mm or 0 mm between the antenna and the water container [20, 44, and 45]. The simulation experiment is conducted by substituting pure water for seawater and distilled water. The reflection coefficients of all cases have finally observed and compared in Figure 14. Since water quality affects the resonance frequency, reflection coefficients, and resonating bands, for each water sample case, the authors have recorded these reflection coefficients at the resonance frequencies. We estimate the antenna quality factor for each water sample [46–49]. The pure water sample achieves the best-estimated antenna sensor quality factor of 21.09, while the sea water has the lowest quality factor of 20.20. Table VI showcases all these data. The shift in resonant frequency as compared to the antenna's resonating frequency in the air is also a significant factor in determining the antenna sensor's numerical sensitivity (NS). The designed antenna sensor is more sensitive to changes in the reflection coefficient value than the antenna's S_{11} in air. This is known as the reflection coefficient (ΔS_{11}) numerical sensitivity. Table VII shows that, compared to the other water samples, it is least sensitive to pure freshwater.

TABLE VI. Antenna quality factor with water samples

Water Sample	f_r (GHz)	$-S_{11}$ (dB)	−10dB Bandwidth f_L-f_H (GHz)	−10dB Bandwidth Δf (GHz)	Quality Factor $Q = \frac{f_r}{\Delta f}$
No water (Antenna in Air)	10.04	21.815	9.7925-10.371	0.5785	17.355
Distilled water	10.08	29.765	9.852-10.316	0.464	21.044
Salt (Sea) water	10.06	39.375	9.837-10.335	0.498	20.20
Pure water	10.06	33.176	9.851-10.328	0.471	21.09

TABLE VII. Sensitivity measurement of the water samples

Water Sample	f_r (GHz)	$-S_{11}$ (dB)	Numerical sensitivity, ΔS_{11} (%)	Change in Δf_r (GHz)	Numerical sensitivity, Freq. NS (%)
No water (Antenna in Air)	10.04	21.815	------	------	-------
Distilled water	10.06	29.545	35.43	0.02	0.198
Salt (Sea) water	10.06	39.375	80.49	0.02	0.198
Pure water	10.08	27.736	27.14	0.04	0.397

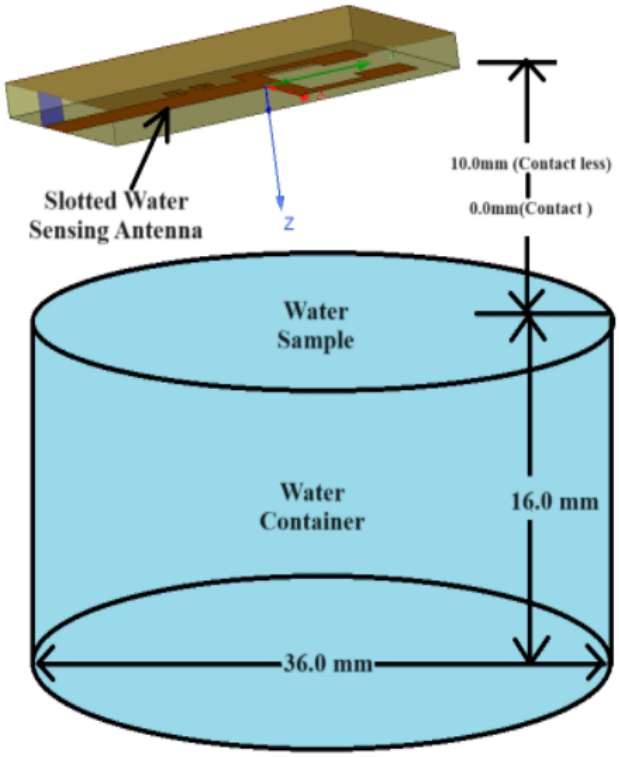

FIGURE 13. Experimental setup for antenna water-sensing system.

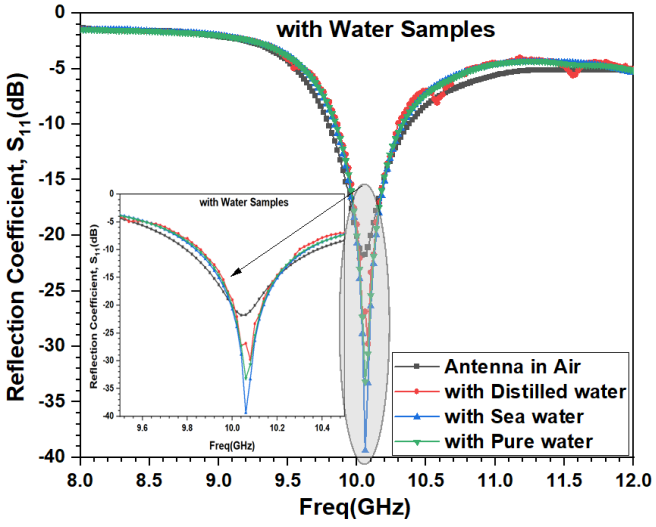

FIGURE 14. Reflection coefficient and resonant frequency sensitivity testing for water samples.

F. ANTENNA SENSITIVITY ANALYSIS

The quality factor (Q) of the antenna sensor is given by:

$$Q = \frac{f_r}{\Delta f} \quad (1)$$

The frequency numerical sensitivity (NS) of the antenna with change in water samples is given by:

$$\text{Frequency NS}\ (\%) = \frac{\Delta f_r}{f_r} \times 100 = \frac{f_r - f_0}{f_r} \times 10 \quad (2)$$

The reflection coefficient numerical sensitivity of the antenna with change in water samples is given by:

Reflection coefficient (S_{11}) NS (%)

$$S_{11}\text{NS}\ (\%) = \frac{\Delta S_{11}}{S_{11-air}} \times 100$$

$$S_{11}\text{NS}(\%) = \frac{S_{(11-air)} - S_{(11-\text{water sample})}}{S_{(11-air}} \times 100 \quad (3)$$

where, f_r and f_0 are resonance frequencies in the air, and with the water sample, respectively.

In this work, the authors conducted two sets of measurements using water samples. One when the antenna is dipped (0.0 mm) inside the water sample, and the other when the distances between the antenna and water samples are kept 10.0 mm apart and the antenna patch faces towards the water container. The first case when the antenna sensor is dipped inside the water sample (0.0 mm contact case) and the second case when the antenna sensor is at a 10.0 mm distance apart (contactless case) from the water sample are shown in Table VIII and Table IX, respectively as displayed in Figure 13.

The sensitivity analysis of the water antenna sensor is estimated in terms of quality factor, reflection coefficient (ΔS_{11}) numerical sensitivity, and resonance frequency NS. From Table VIII recorded data, where $\Delta f_r = f_r - f_0$ (f_r is the resonant frequency of the sensing antenna in air, and f_0 is the resonant frequency of the sensing antenna with water samples). The sensor's measured resonant frequency is 10.10 GHz. Further, from Figure 15, the measured resonant frequencies of the sensor with spring water, fountain water, salt water, and distilled water samples are 10.24 GHz, 10.22 GHz, 10.10 GHz, and 10.26 GHz, respectively.

TABLE VIII. Contact case: Antenna Dipped case in Water sample (0.0 mm).

Water Sample with TDS value	f_r (GHz)	$-S_{11}$ (dB)	−10dB BW $\Delta f = f_L - f_H$ (GHz)	Quality factor, Q	ΔS_{11} NS (%)	$\Delta f_r = f_r - f_0$ (GHz)	Freq. NS (%)
No water (Ant. in Air)	10.10	20.23	0.14 (10.02-10.16)	72.143	------	------	-----
Spring water (129)	10.24	23.173	0.12 (10.17-10.29)	85.33	14.54	0.14	1.386
Fountain Water (282)	10.22	15.982	0.10 (10.17-10.27)	102.2	20.99	0.12	1.188
Salt (Sea) water (981)	10.10	15.494	0.12 (10.05-10.17)	84.17	23.41	0.00	0
Distilled water (28)	10.26	14.22	0.18 (10.13-10.31)	57	29.708	0.16	1.584

*Note: f_r= Resonating frequency; S_{11} = Reflection Coefficient; BW=bandwidth; Q= Quality Factor; f_o=

Resonance frequency of antenna in air; NS=Numerical sensitivity.

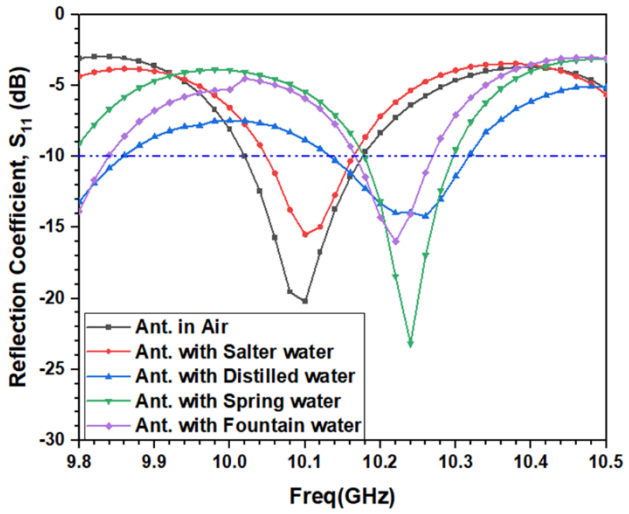

FIGURE 15. Water sensing antenna reflection coefficients measurement at 0mm distance from water samples level.

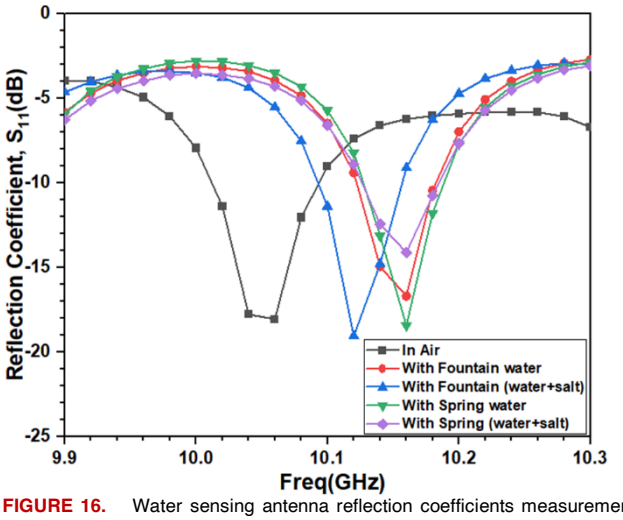

FIGURE 16. Water sensing antenna reflection coefficients measurements with water samples at 10mm distance from water samples level.

Furthermore, we estimate the NS of the sensor, defined as the percentage change in resonant frequency compared to the resonant frequency concerning the resonant frequency of the antenna in the air. The estimated values of numerical sensitivity (NS) for the samples are 1.386%, 1.188%, 0%, and 1.584%, respectively, this applies to spring, fountain, salt, and distilled water samples. Therefore, in this dipped case, the antenna is almost insensitive to the resonant frequencies. On the other hand, the values of the reflection coefficients were observed to be highly sensitive with water samples. Similarly, for the second case measurement, when the antenna distance is 10.0 mm from water samples the resonant frequency NS almost lies between 0% and <1%. This again verifies that the antenna is less sensitive to resonant frequency changes while it is greatly sensitive to the change in reflection coefficients with water samples. Table IX shows the measured NSs of the proposed sensor concerning the resonant frequency and reflection coefficients in the second case, and their reflection coefficients are shown in Figure 16.

TABLE IX. Contactless case: Antenna undipped case in Water sample (10.0 mm) with water samples at 10.0mm distance.

Water Sample with TDS (PPM)	f_r (GHz)	$-S_{11}$ (dB)	-10dB BW $\Delta f = f_L - f_H$ (GHz)	Quality factor, Q	ΔS_{11}NS (%)	$\Delta f_r = f_r - f_0$ (GHz)	Freq. NS (%)
No water (Antenna in Air)	10.06	18.06	0.081 (10.012 - 10.093)	124.20	------	-------	---- ----
Spring water (129)	10.16	18.427	0.061 (10.127 - 10.188)	166.55	2.03 (Excellent For drinking)	0.10	0.994
Spring (water +salt) water (981)	10.16	14.118	0.057 (10.126 - 10.184)	178.24	21.827	0.10	0.994
Fountain Water (282)	10.16	16.692	0.06 (10.13-10.19)	169.33	7.575	0.10	0.994
Fountain (water +salt) water (981)	10.12	19.06	0.08 (10.09-10.17)	126.5	5.537	0.06	0.593

*Note: f_r= Resonating frequency; S_{11} = Reflection Coefficient; BW=bandwidth; Q= Quality Factor; f_o= Resonance frequency of antenna in air; NS=Numerical sensitivity; Freq.=Frequency

G. CONTACT VS CONTACTLESS CASE WITH WATER SAMPLE TDS VALUES

The reflection coefficient numerical sensitivity (ΔS_{11} NS) histogram plots of the contact and contactless cases with contact (i.e., 0 mm) and contactless (i.e., 10 mm) antenna sensors from the water levels are shown in Figure 17. The water samples TDS values are considered same for both the cases and the numerical sensitivity of the reflection coefficient of both the cases have been analyzed. When the designed antenna is dipped inside the water, the reflection coefficient numerical sensitivity is higher for the contact case as displayed by red colored histograms, and the reflection coefficient NS values decreases as the distance of the antenna is kept 10 mm from different water samples (contactless case). The experiment displays these reflection coefficient numerical sensitivities in relation to the measured TDS values of distilled water, spring water, fountain water, and salted water. The measured values of the TDS of different water samples are 28 PPM (Distilled water), 129 PPM (Spring Water), 282 PPM (Fountain Water), and 981 PPM (Salted water), respectively for both contact and contactless cases. These TDS represent the water's hardness in terms of the total dissolved solids

present in it, i.e., sodium, calcium, magnesium, phosphorus, potassium, carbonates, nitrates, bicarbonates, chlorides, sulfates, and so on. The distilled water contains minerals and nutrition, and its TDS value is <30 PPM; therefore, it does not provide any health benefits. Water with a TDS value between 50 and 150 PPM is excellent for drinking. Water with TDS values of 150–250 PPM is good to drink; water with 250–300 PPM is fair to drink. The TDS value of 300–500 PPM is poor quality and therefore not acceptable for drinking. Drinks should not contain TDS levels exceeding 1200 PPM. Experiment can extract the reflection coefficient sensitivity from the TDS values of the water and vice versa based on the numerical sensitivity of the reflection coefficients ranges. The histograms show that the water samples with a low reflection coefficient sensitivity (<10%) are excellent for drinking and have lower TDS values, whereas the water samples with a high reflection coefficient numerical sensitivity (>10%) are not good for drinking. Spring water and fountain water are the best options for healthy drinking water as with available TDS values these water samples reflection coefficients numerical sensitivities (in case of contactless case with 10 mm antenna distance from water level) are very close to the regression line. This is also true with TDS value of these water samples between 100 PPM to 300 PPM as shown in Figure 15a.

The reflection coefficients numerical sensitivity of contact case and contact less case are tested using the regression line analysis as illustrated in Figures 17b and 17c. For contact case the water samples points are away from the regression line and regression coefficient shows coefficient of determination (R^2) value 0.517 [Figure 17b] that is corresponds to poor linear relationship as the reflection coefficients numerical sensitivity samples are existing much far away from the regression line and therefore contact case ΔS_{11} NS shows non-linearity behavior with the water TDS values. Similarly, for second contactless case the R^2 value is 0.83 that is close to 1 (perfect value) [Figure 17c]. This value shows strong linear relationship between contactless reflection coefficients numerical sensitivity of water samples and regression line. Therefore, it is concluded that contactless case of water sample with TDS is more sophisticated as compared to contact case water samples.

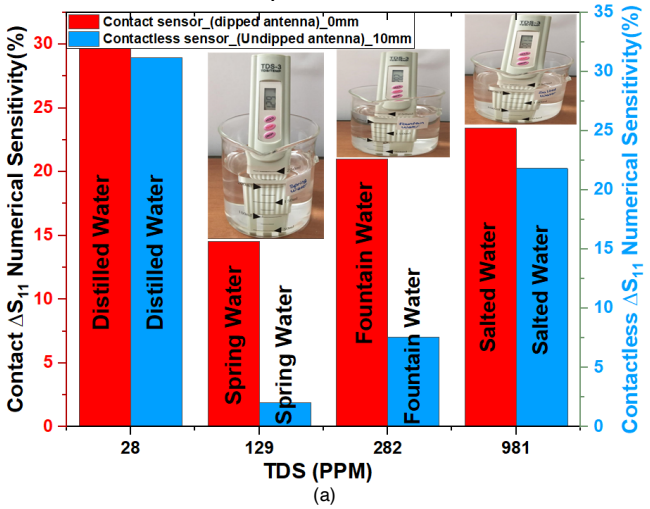

(a)

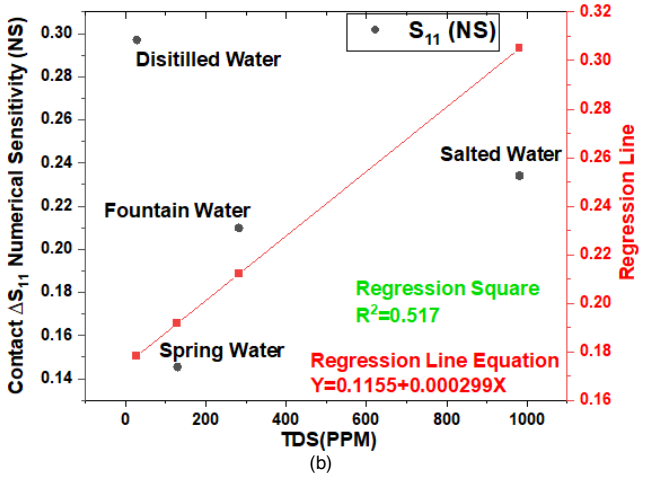

(b)

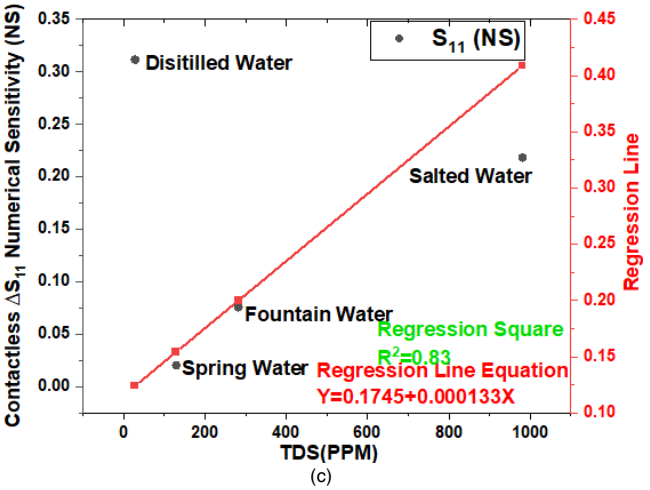

(c)

FIGURE 17. Contact and contactless ΔS_{11} numerical sensitivity of water sensing antenna from water level [with contact (0.0mm) and contactless (10.0 mm)] (a) ΔS11 NS with water sample TDS, (b) Regression analysis of contact case, and (c) Regression analysis of contactless case.

H. FREQUENCY SHIFTING WITH WATER CONTAINER DISTANCE FROM THE ANTENNA

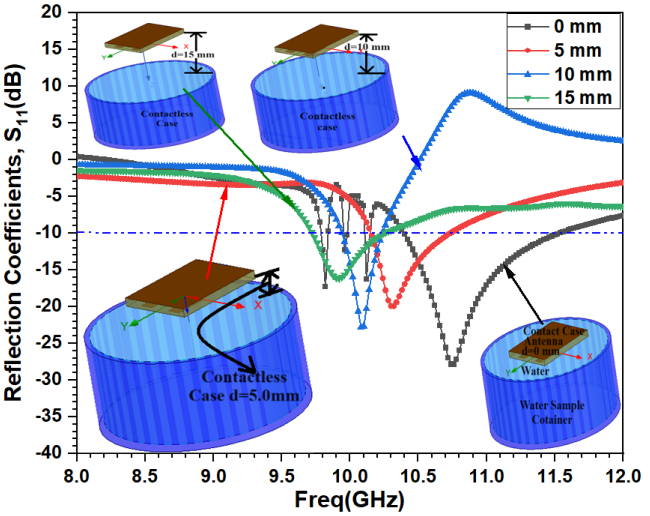

(a)

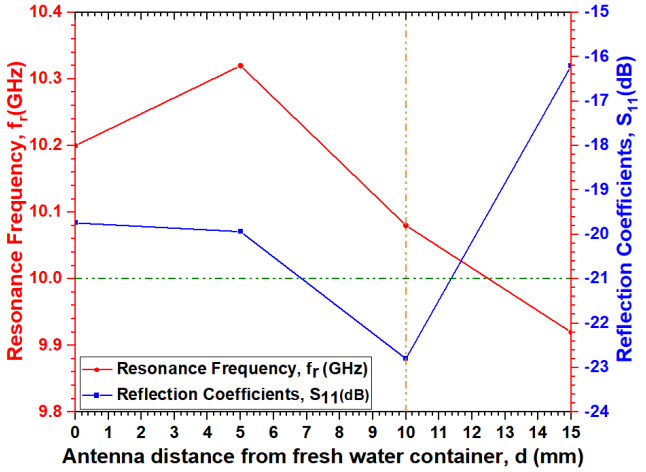

(b)

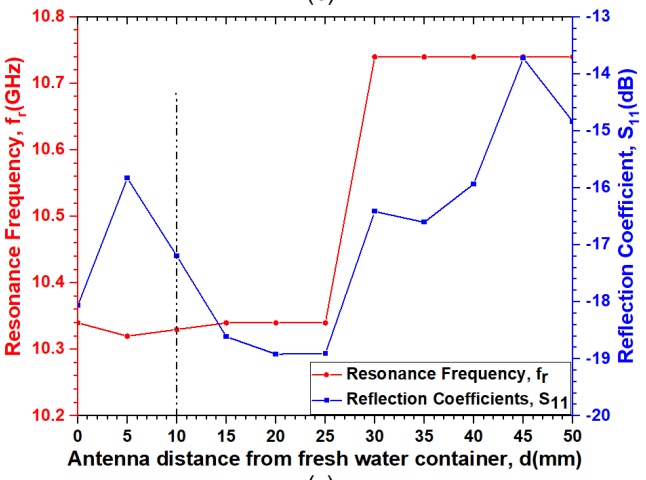

(c)

FIGURE 18. Effect of water sample distance on resonance frequency shift and change in reflection coefficient

The authors have analyzed a new parametric test experiment about the antenna's proximity to the freshwater container. In steps of 5 mm, the authors vary the antenna's distance from the filled water sample container from 0 mm to 15 mm. Figure 18a represents the numerical simulated parametric study of the distance. This means that as the distance between the water sample level and antenna decreases from 15 mm to 0 mm, the resonance frequency shifts away from the 10 GHz frequency, and vice versa. Therefore, for a gap (d) of 10.0 mm, we achieve excellent reflection coefficients of -26.88 dB at a frequency of 10 GHz. As the distance increases from 10 mm to 15 mm, the reflection coefficient deteriorates, and the resonance frequency shifts leftward from the 10 GHz resonant frequency. There are two linearity plots. In Figure 18b they show how the measured resonance frequency (f_r) and the reflection coefficients (S_{11} variation) change as the distance between the antenna and the water sample container changes. The results show that a 10 mm gap (d) between the water sample level and the antenna has an excellent reflection coefficient and a resonance frequency close to the 10 GHz operating frequency. The authors further analyzed the contactless case using a hardware experimental setup, varying the distance from 0 mm to 50 mm in 5 mm steps, as shown in Figure 18c. It is evident from Figure 18c that a distance of 10 mm to 25 mm is best suitable for the operation to test the water sample using an antenna, as it received the closest resonance frequency of 10 GHz and good reflection coefficient values below -10 dB.

The overall parametric study concludes that the contactless method of measuring a water sample outperforms the contact method using an antenna sensor.

I. EFFECT OF WATER SAMPLE TEMPERATURE ON RESONANCE FREQUENCY AND REFLECTION COEFFICIENT

Water's electrical properties are highly dependent on temperature. Therefore, it is important to consider the effect of water sample temperature on the resonance frequency and reflection coefficient antenna performance parameters. Figure 19 represents the effect of water temperature changes on the antenna resonance frequency shifts and reflection coefficient changes. The linearity plots with temperature indicate that the frequency shifts vary between 10.18 GHz and 11.32 GHz, and the reflection coefficient varies between -12.5 dB and -33 dB as the temperature rises from 0°C (refrigerator water) to 100°C (boiled water). The authors took each experimental measurement with a 10°C step change in temperature. They observed the closest resonance frequency with an acceptable reflection coefficient at room temperature (27°C). The two linear plots of resonance frequency (f_r), and reflection coefficients (S_{11}) dependent on the temperature of the water sample. These two linear equations are derived using curve fitting method;

$$f_r = 8.546 \times 10^6 T + 10.4 \times 10^9$$

i.e., $$f_r(GHz) = 0.0085T + 10.4 \quad (4)$$

$$S_{11}(dB) = -0.05T - 15.05 \quad (5)$$

Where, T is the temperature of water sample in °C. Equation 4 ascribed that 1°C rise in temperature increases the resonance frequency by 0.4085 GHz right from the frequency 10 GHz. Beside this Equation 5 ascribed that 1°C rise in temperature decreases the improves the reflection coefficient by -0.05 dB from -15.05 dB value.

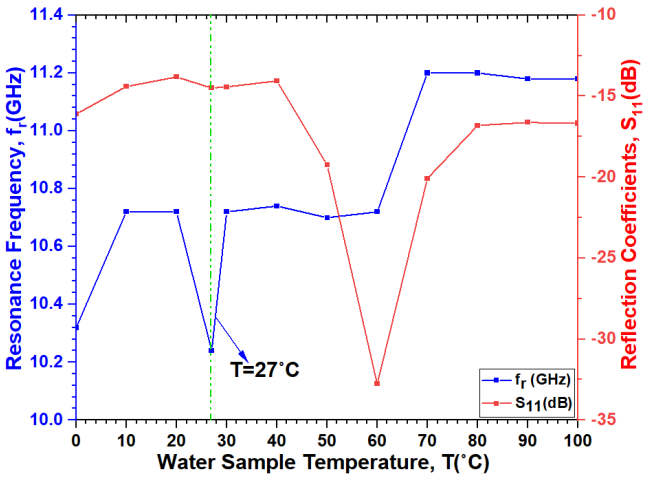

FIGURE 19. Effect of water sample temperature on resonance frequency shift and change in reflection coefficient

J. PROPOSED ANTENNA COMPARISON WITH SIMILAR EXISTING LITERATURE

The state-of-the-art comparison of the proposed antenna with the similar types of existing water sensing antennas have been summarized in Table X. The proposed antenna is compact in size, cumbersome, offset-feed, and low-cost. Simple structure makes its fabrication easy as compared to complex structured reported antennas. The reported antenna is used for the water sensor, but it is not limited to water-sensing elements, the same antenna could be used for a sensor for milk quality, raw spices, flour, juice, liquid as well as solid food quality evaluation and analysis, etc.

The antenna is excellent choice as liquid sensor to examine any chemical, juice, blood etc. on the basis of evaluated sensitivity parameters. This is the only work that consider all the sensitivity analysis and regression analysis none of the reported literature antenna used two cases and analyzed all sensitivity parameters.

TABLE X. State-of-the-art comparison with existing water sensing antennas.

Ref. (year)	f_r (GHz)	Permittivity	sensor	Contact (d)	Sample size	Antenna Size (mm^3)	Frequency shift (MHz)	Reflection Coefficient Shift (dB)	Δf_r (NS) (%)	ΔS_{11} (NS) (%)	R^2
Proposed work	10	4.4	Slotted antenna	yes (0 mm)	100mL	18.65×14×1.6	140	-2.897	1.386	14.54	0.517
Proposed work	10	4.4	Slotted antenna	No (10 mm)	100mL	18.65×14×1.6	400	3.88	0.997	2.03	0.83
[14] Aiswarya et al. (2023)	2.48	4.4	Loop antenna	Yes (0 mm)	25µL	38.8× 38.8 ×1.6	600	9.7	----	13.7	----
[18] El-Nady et al. (2024)	4-11	10.2	ENZ Metamaterial Microwave Sensor (Vivaldi antenna)	Yes (Dipped case)	100mL	51.3× 42.9 ×1.27	----	0.3	----	1	----
[20] Vinoth et al. (2023)	3.5	4.4	Planar Edged UWB Antenna	Yes (Dipped case)	100mL	30×35× 1.6	300	7.8	----	----	----
[35] Al-Gburi et al., (2023)		2.5	Triple-Rings CSRR Microwave Sensor	Yes (0 mm)	7.92 µL	20 × 25 × 1.52	340	0.63	----	----	----
[45] Logeswaran and Rani (2022)	5.3	4.4	Rectangular patch with stepped structure	Yes (Dipped case)	150 mL	33.7 × 27.5× 0.8	120	2.83	---	---	---
[47] Nitika, Kaur J et al. (2023)	4-18	4.4	Rake-shaped microstrip sensors	Yes (Dipped case)	200mL	30×27×1.57	220	11	---	---	---
[49] Javed et al. (2020)	2.0	4.4	CSRR based transmission line	No	-----	35×25×1.5	379	2	---	---	---

Aiswarya et al. (2023) present a larger size and lower frequency (2.48 GHz) for primarily milk analysis. It is concluded to have an adequate reflection coefficient for milk but is less suitable for higher-frequency applications [14]. El-Nady et al. (2024) depict the larger size, multi-frequency operation (8, 9, 11 GHz) for water with salt and sugar. However, the performance is good for a variety of water impurities, despite its bulkiness [18]. Vinoth et al. (2023) investigate larger-size, multi-frequency operations for distilled, RO, and raw water. It is versatile for multiple water types but larger in size [20]. Abdulkarim et al. (2020) focus on larger sizes and lower frequencies (1.9 GHz) for water, methanol, ethanol, and oil. The proposed antenna is effective for various liquids, including oils, but has a has a lower frequency [31]. Al-Gburi et al. (2023) propose a smaller size and a lower frequency (2.5 GHz) for specific food items like turmeric and ginger. The proposed structure targets specific items and limited water applications [35]. Alhawari et al. (2021) possess much larger size, multi-frequency operation along with fresh, distilled, and sea water. The performance is acceptable for extensive water quality analysis, but impractically large [50]. Whayan & Vyas (2020) underpin the much larger size, lower frequency (1.62 GHz) for water with sugar and salt. The proposed structure is specific to certain water types, too large for practical use [50]. Nitika et al. (2022) [46] study smaller size, slightly higher frequency (10.66 GHz) for different milk types. The antenna is promising structure for milk but limited to this application [46]. Nitika et al. (2023) [47] depicts larger size, higher frequency (14.32 GHz) for water and juice with various additives. The structure is suitable for diverse liquids, larger size [47]. Nitika et al. (2022) [48] design smaller size, higher

frequency (13.3 GHz) for common raw spices. The antenna is optimized for spices, less for water [48]. Javed et al. (2020) [49] study larger size, lower frequency (2.45 GHz) for water with various alcohols. The performance of the antenna is effective for alcohol mixtures, larger size [49].

This study focuses on compact size (18.65×14×1.6 mm³), optimized frequency (10.0 GHz) for Various water qualities (Sea, Distilled, Fountain, Spring, Pure). The simulation and measurement results depict that the proposed antenna structure yields high quality factor, superior sensitivity and specificity, compact and versatile design. In this study, the proposed antenna stands out in several key areas when compared to the antennas listed above:

Compact Design: With a size of 18.65×14×1.6 mm³, our antenna is significantly more compact than most other designs. This compactness makes it highly suitable for integration into portable and space-constrained applications.

Optimized Frequency: Operating at 10.04 GHz, our antenna is specifically optimized for water quality sensing. Higher frequencies, like ours, provide better resolution and sensitivity, which are crucial for detecting subtle differences in water composition.

Targeted Application: Unlike many other antennas that cater to a broad range of applications, our antenna is tailored specifically for water quality sensing. This specialization ensures higher accuracy and reliability in detecting various water qualities, including sea, distilled, fountain, spring, and pure water.

Enhanced Sensitivity and Specificity: Our antenna demonstrates superior sensitivity and specificity, making it highly effective for environmental monitoring and public health applications. The high-quality factor and optimized S_{11} parameter ensure precise measurements.

Addressing a Research Gap: There is a recognized gap in the development of antennas optimized for water quality sensing. Our study addresses this gap by providing a detailed design and analysis of an antenna that meets the specific needs of this application, setting a new benchmark for future research.

In conclusion, the proposed antenna offers a unique combination of compactness, optimized frequency, targeted application, and superior performance metrics. These advantages highlight its potential impact on advancing.

IV. CONCLUSION

This study presents a novel slotted split ring-loaded rectangular patch low-cost antenna as a water quality sensing element. The research evaluated and analyzed the performance of the water-sensing antenna using different water samples, such as seawater, distilled water, pure water, fountain water, spring water, and salted water. The authors designed, fabricated, and evaluated the sensor experimentally. The sensor presented a reflection coefficient of −21.815 dB and a resonant frequency of 10.04 GHz. The simulated and measured results for the sensing antenna's reflection coefficient and radiation patterns agree very well, which proves that the proposed sensor is a sensitive way to find out about water quality. The proposed antenna has a Q-factor of 74.143, and the reflection coefficient NS for pure water is 27.14%. It is concluded that pure water and distilled water are less sensitive to the reflection coefficient, while salted drinking water (high TDS) is highly sensitive to the reflection coefficient value at resonating frequency. Furthermore, the antenna has a resonant frequency sensitivity of less than 1.5%. Consequently, the reflection coefficient sensitivity enables the observation of a change in water quality TDS level. Water samples interact with the electromagnetic field through shifts in resonant frequency and changes in their reflection coefficient values, enabling the practical examination of the proposed antenna-based sensor for water sample distinction. The variable discrepancy of the reflection coefficient with different water samples increases or decreases depending on the type of TDS present in the water or its hardness. The proposed sensor detects a specific percentage of TDS levels and doesn't require harmful chemicals or an expensive setup, ensuring speedy performance and simple estimation. The simple structure of the proposed sensor facilitates its fabrication, unlike the complexly structured reported antennas. The reported antenna is used for the water sensor, but it is not limited to the water sensing element; the same antenna could be used for a sensor for milk quality, raw spices, flour, juice, liquid, as well as solid food quality evaluation and analysis, etc. This antenna's selection of X-band design frequency makes it suitable for performing experiments in microwave laboratories in technical universities, as X-band setups are generally available there.

REFERENCES

[1] M. Yildirim, M.A. Gözel, "Asimetrik eş-düzlemsel şerit beslemeli anten ile motor yağ seviye ve kullanim ömrü tespiti," *Mühendislik Bilimleri ve Tasarım Dergisi*, 11(3), 904-915 (2023).

[2] Y. Rahmat-Samii, E. Topsakal, "*Antenna and sensor technologies in modern medical applications*," Wiley-IEEE (2021).

[3] S. M. Ali, C. Sovuthy, S. Noghanian, T. Saeidi, M. F. Majeed, A. Hussain, Q.H. Abbasi, "Design and evaluation of a button sensor antenna for on-body monitoring activity in healthcare applications," *Micromachines*, 13(3), 475 (2022).

[4] W. Wang, X. W. Xuan, W. Y. Zhao, H. K. Nie, "An implantable antenna sensor for medical applications," *IEEE Sensors Journal*, 21(13), 14035-14042 (2021).

[5] A. Sabban, "Wearable circular polarized antennas for health care, 5G, energy harvesting, and IoT systems," *Electronics*, 11(3), 427 (2022).

[6] M. El Gharbi, R. Fernández-García, S. Ahyoud, I. Gil, "A review of flexible wearable antenna sensors: design, fabrication methods, and applications," *Materials*, 13(17), 3781 (2020).

[7] V. Satam, C. Kulkarni, A. Kholapure, "Microstrip Antenna as a Temperature Sensor for IoT Applications," IEEE Microwaves, Antennas, and Propagation Conference (MAPCON), Bangalore, India, 944-947 (2022).

[8] R. Kozak, K. Khorsand, T. Zarifi, K. Golovin, M.H. Zarifi, "Patch antenna sensor for wireless ice and frost detection," *Scientific Reports*, 11(1), 13707(2021).

[9] H. Sterner, W. Aichholzer, M. Haselberger, "Development of an antenna sensor for occupant detection in passenger transportation," Procedia Engineering, 47, 178-183(2012).

[10] M. A. U. Haq, A. Armghan, K. Aliqab, M. Alsharari, "A Review of Contemporary Microwave Antenna Sensors: Designs, Fabrication Techniques, and Potential Application," IEEE *Access*, 11, 40064-40074 (2023).

[11] M. T. Islam, F. B.Ashraf, T. Alam, , N. Misran, K. B.Mat, "A compact ultrawideband antenna based on hexagonal split-ring resonator for pH sensor application," *Sensors*, 18(9), 2959(2018).
[12] F. M. Tchafa, H. Huang, "Microstrip patch antenna for simultaneous strain and temperature sensing," *Smart Materials and Structures*, 27(6), 065019 (2018).
[13] J. Kaur, R. Khanna, "Graphene based T-shaped monopole antenna sensor for food quality evaluation,". *Journal of the Science of Food and Agriculture* (2024). https://doi.org/10.1002/jsfa.13272
[14] S. Aiswarya, L. Meenu, K. U. Menon, M. Donelli, S. K. Menon, "A Novel Microstrip Sensor Based on Closed Loop Antenna for Adulteration Detection of Liquid Samples," *IEEE Sensors Journal* (2023).
[15] J. Kaur, R. Khanna, "Rake-shaped microstrip sensors with high spatial resolution for analyzing liquid food quality," *International Journal of Microwave and Wireless Technologies*, 15(2), 204-212 (2023).
[16] J. A. I. Araujo, I. Llamas-Garro, Z. Brito-Brito, F. Mira, X. Artiga, M. T. De Melo, "Non-invasive antenna sensor for dielectric material identification at a distance," *Measurement*, 224, 113842 (2024).
[17] R. Raju, G. E. Bridges, S. Bhadra, "Wireless passive sensors for food quality monitoring: Improving the safety of food products," *IEEE antennas and propagation magazine*, 62(5), 76-89 (2020).
[18] S. El-Nady, A. Afifi, A. El-Hameed, S. Anwer, "Sugar and Salt Concentration Detection in Water Employing ENZ Metamaterial Microwave Sensor," *Wireless Personal Communications*, 1-20 (2024).
[19] S. K. Menon, M. Donelli, "Development of a microwave sensor for solid and liquid substances based on closed loop resonator," *Sensors*, 21(24), 8506 (2021).
[20] J. C. Vinoth, S. Ramesh, Z. Z. Abidin, S. A. Qureshi, E. Saranya, M. Josephine, G. Sneha, "Planar edged UWB antenna for water quality measurement," *Progress In Electromagnetics Research*, 130, 83-93(2023).
[21] N. Meyne, S. Latus, A. F. Jacob, "Corrugated Coplanar Transmission-Line Sensor for Broadband Liquid Sample Characterization," German Microwave Conference, Aachen, Germany, 1-4 (2014).
[22] W. Withayachumnankul, A. Tuantranont, C. Fumeaux, D. Abbott, "Metamaterial-based microfluidic sensor for dielectric characterization," *Sensors and Actuators A: Physical*, 189, 233-237 (2013).
[23] N. Meyne, C. Cammin, A. F. Jacob, "Accuracy enhancement of a split-ring resonator liquid sensor using dielectric resonator coupling," 20th International Conference on Microwaves, Radar, and Wireless Communications (MIKON), Gdansk, Poland, 1-4 (2014).
[24] A. A. Al-Mudhafar, A. M. Ra'ed, "High-precise microwave active antenna sensor (MAAS) formulated for sensing liquid properties," *Sensors and Actuators A: Physical*, 341, 113567 (2022).
[25] O. AKGÖL, "PCB Dairesel Yama Anten Tabanlı Etanol ve Metanol Algılayıcı Tasarımı," *Çukurova Üniversitesi Mühendislik-Mimarlık Fakültesi Dergisi*, 33(2), 287-296(2018).
[26] A. Bouchalkha, R. Karli, "Planar Microstrip Antenna Sensor for pH Measurements," International Conference on Electrical and Computing Technologies and Applications (ICECTA) 1-5 (2019).
[27] K. Lee, A. Hassan, C. H. Lee, J. Bae, "Microstrip patch sensor for salinity determination," *Sensors*, 17(12), 2941 (2017).
[28] L. Zhu, W. Li, X. Han, Y. Peng, "Microfluidic flexible substrate integrated microstrip antenna sensor for sensing of moisture content in lubricating oil," *International Journal of Antennas and Propagation*, 1-9 (2020).
[29] A. Tamer, "İletim hatları ve metamalzemeler kullanılarak legal–illegal benzin ve mazot ayrıştırılması," M.S. thesis, Department of Electrical-Electronics Engineering, İskenderun Technical University, 2019.
[30] E. L. Chuma, Y. Iano, G. Fontgalland, L. L. B. Roger, "Microwave sensor for liquid dielectric characterization based on metamaterial complementary split ring resonator," *IEEE Sensors Journal*, 18(24), 9978-9983 (2018).
[31] Y. I. Abdulkarim, L. Deng, M. Karaaslan, O. Altıntaş, H. N. Awl, F. F. Muhammadsharif, H. Luo, "Novel metamaterials-based hypersensitized liquid sensor integrating omega-shaped resonator with microstrip transmission line," *Sensors*, 20(3), 943 (2020).
[32] N. Meyne née Haase, G. Fuge, H. K. Trieu, A. P. Zeng, A. F. Jacob, "Miniaturized Transmission-Line Sensor for Broadband Dielectric Characterization of Biological Liquids and Cell Suspensions," *IEEE Transactions on Microwave Theory and Techniques*, 63, 10, 3026-3033 (2015).
[33] Ş. Dalgaç, F. Karadağ, M.Bakır, O. Akgöl, E. Ünal, M. Karaaslan, "Chiral metamaterial-based sensor applications to determine quality of car lubrication oil," *Transactions of the Institute of Measurement and Control*, 43(7), 1640-1649 (2021).
[34] M. BAKIR, İ. YASAR, "Metamalzeme Tabanlı Hassas Süt ve Sıvı Sensörü Uygulaması," *Avrupa Bilim ve Teknoloji Dergisi* 10-16 (2020).
[35] A. J. A. Al-Gburi, N. A. Rahman, Z. Zakaria, M. Palandoken, "Detection of semi-solid materials utilizing triple-rings CSRR microwave sensor," *Sensors*, 23(6), 3058 (2023).
[36] M. H. Bhatti, M. A. Jabbar, M. A. Khan, Y. Massoud, "Low-cost microwave sensor for characterization and adulteration detection in edible oil," *Applied Sciences*, 12(17), 8665 (2022).
[37] K. S. L. Parvathi, S. R. Gupta, "Ultrahigh-Sensitivity and Compact EBG-Based Microwave Sensor for Liquid Characterization," *IEEE Sensors Letters*, 6(4), 1-4 (2022).
[38] C. Balanis, "Antenna Theory and Design", New Delhi:McGraw Hill, 2003.
[39] A.P.S. Pharwaha, J. Singh, T.S. Kamal,"Estimation of feed position of rectangular microstrip patch antenna," IE Journal-ET Volume, vol. 91, (2010).
[40] J.S. Sivia, A.P. S. Pharwaha, T.S. Kamal, "Design of sierpinski carpet fractal antenna using Artificial Neural Network," International *Journal of Computer Application*, 68(8), 5-10(2013).
[41] J.S. Sivia, S.S. Bhatia, "Design of fractal based microstrip rectangular patch antenna for multiband applications," IEEE International Advance Computing Conference (IACC), 712-715 (2015).
[42] A. K. Sidhu, J. S. Sivia, "Microstrip Rectangular Patch Antenna for S and X band applications," International Conference on Wireless Communications, Signal Processing and Networking (WiSPNET), Chennai, India, 248-251 (2016).
[43] U. Kaatze, and V. Uhlendorf, "The Dielectric Properties of Water at Microwave Frequencies," Zeitschrift für Physikalische Chemie, 126 (2), 151-165, 1981.
[44] R.C. Mahajan, V. Vyas, "Wideband microstrip antenna for the detection of solutes in water," *Engineering Reports*, 2021.
[45] J. Logeswaran, R.B. Rani, "UWB Antenna as a Sensor for the Analysis of Dissolved Particles and Water Quality," *Progress in Electromagnetics Research Letters*, Vol. 106, 31-39, 2022.
[46] Nitika, J. Kaur, R. Khanna, "Novel monkey-wrench-shaped microstrip patch sensor for food evaluation and analysis," J *Sci Food Agric.*, 15;102(4):1443-1456, 2022. Mar. doi: 10.1002/jsfa.11478. Epub 2021 Aug 31. PMID: 34390496.
[47] Nitika, J. Kaur, R. Khanna, "Rake-shaped microstrip sensors with high spatial resolution for analyzing liquid food quality," International Journal of Microwave and Wireless Technologies 15, 204–212, 2023. https://doi.org/10.1017/S1759078722000587
[48] Nitika, J. Kaur, R. Khanna, "Exploration of adulteration in common raw spices using antenna-based sensor," International Journal of Microwave and Wireless Technologies 1–13, 2022. https://doi.org/10.1017/S175907872200112X
[49] A. Javed, A. Arif, M. Zubair, "A low-cost multiple complementary split-ring resonator-based microwave sensor for contactless dielectric characterization of liquids," IEEE Sensors Journal 20, 11326–11334, 2020.
[50] A.R.H. Alhawari, S.F. Majeed, T. Saeidi, S. Mumtaz, H. Alghamdi, A.T. Hindi, A.H.M. Almawgani, M.A. Imran, Q.H. Abbasi, "Compact Elliptical UWB Antenna for Underwater Wireless Communications," *Micromachines*, 12, 411, 2021
[51] S. Singh, A. Varshney, V. Sharma, I. Elfergani, C. Zebiri, & J. Rodriguez, "A Compact Off-Set Edge Fed Odd-Symmetric Hybrid Fractal Slotted Antenna for UWB and Space Applications," Progress in Electromagnetics Research B, 102, 2023.
[52] F.F. Sousa, L.D. Silva, and K.H. Freitas, "Electrical and dielectric properties of water," *Scientia Plena, 13, 1, 1-6, 2017*.